

NUMERICAL STUDY ON THE NEAR-FIELD BEHAVIOR OF 3-D LINE INCLINED POSITIVELY BUOYANT JETS IN CROSS FLOWS

Jimin HU¹, Jianlong GU² and Huiling HAN³

¹ Institute of Water Resources and Flood Control, Dalian University of Technology, Dalian, Liaoning Province 116024, China. Phone: 0086-0411-81743629 E-Mail: jimihu_2004@yahoo.com.cn

² Institute of Environment Engineering Research, Dalian Maritime University, Dalian 116026, China

³ School of Urban and Rural Construction, Hebei Agriculture University, Baoding 071001, China

ABSTRACT

This paper presents the results of a numerical calculation on the near-field behavior of three-dimensional (3-D) line inclined positively buoyant jets of slot with width B and length $L = 4B$, discharge into relatively deep uniform cross flows at angle of 60° to the horizontal. The R , which is the ratio of ambient velocity to jet exit velocity, is varied from 0.2 to 0.6 and influences specific properties of the flow. The calculations are performed with the standard $\kappa - \varepsilon$ model and the Hybrid Finite Analytic Method (HFAM) and staggered grid. The phenomenon and development of vortex pairs are simulated successfully and influence of R on turbulent buoyant jets is analysed.

NOMENCLATURE

B width of slot
 $C_\mu, C_{\varepsilon 1}, C_{\varepsilon 2}, \sigma_k, \sigma_\varepsilon$ constants in $\kappa - \varepsilon$ model
 E roughness parameter
 F_j discharge densimetric Froude number
 g_i gravitational acceleration
 h, k, l distances between two grid points in x, y, z direction.
 K von Karman constant
 L length of slot
 P intensity of pressure
 P_k production of the turbulent kinetic energy
 p_{rt} turbulent Prandtl number
 R ratio of ambient velocity to jet exit velocity
 T temperature of jets
 T_0 jet exit temperature
 T_a temperature of uniform cross flows
 u, v, w three-dimensional velocities
 u_i mean velocity component in x_i direction
 u'_i fluctuating velocity component in x_i direction
 u_a velocity of uniform cross flows
 u_p resultant velocity parallel to the wall
 u_* resultant friction velocity
 W_0 jet exit velocity
 X, Y, Z Cartesian coordinate system with Z upword
 x_i co-ordinates in tensor notation
 y_p distance between the first grid and wall
 y^+ dimensionless wall distance

α heat expansion coefficient
 δ_{ij} Kronecker delta, =1 for $i = j$ and =0 for $i \neq j$
 ε dissipation rate of κ
 θ jet exit velocity angle relative to horizontal
 ν kinematic viscosity
 ν_t teddy viscosity
 ρ_a ambient fluid density
 κ turbulent kinetic energy

INTRODUCTION

With the development of human society, environment has become an urgent issue in the world. If jets through finite-length slot or multipoint diffuser that is frequently designed with nozzles spaced so closely discharge effluent coming from industry or agriculture into moving flows, this kind of jets can be generalized as line turbulent buoyant jets in moving flows. Generally, if θ (the jet exit velocity angle relative to horizontal) equals 90° , the jet is called line perpendicular turbulent buoyant jets in moving flows; if θ equals 0° , the jet is called line horizontal turbulent buoyant jets in moving flows; if θ doesn't equal 90° and 0° , the jet is called line inclined turbulent buoyant jets in moving flows (HU and HAN, 2004). Water quality standards require high dilutions within a limited mixing zone (JIRKA, 1982), and the purpose of this strategy of environmental conservation is to constrain the impact of heated discharges to a small area. Finite length line inclined positively buoyant jets in uniform cross flows is a basic flow shape of environmental pollution. The dilution effect of it is superior to perpendicular jets for smaller R and lower cross flows (HU and HAN, 2004). Therefore, numerical simulation on it can provide theoretical basis to design discharge-into-sea diffusers, which is of great theoretical value and practical meaning.

MATHEMATICAL MODEL

The configuration considered in this study is described in Figure 1. The thermal jets for temperature is T_0 and velocity is W_0 is discharged into a relatively deep uniform cross flow which of temperature is T_a and velocity is u_a from a slot with width B and length L at angle of 60° to the horizontal ($T_0 > T_a$). The standard $\kappa - \varepsilon$ turbulent model, staggered grid and Hybrid Finite Analytic Method (LI, 2000) are adopted in the present study.

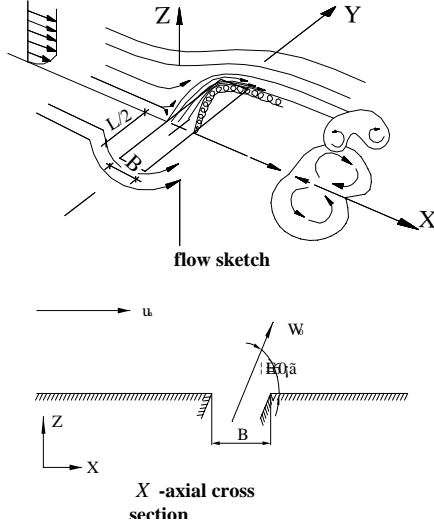


Figure 1: Diagram of finite length line inclined positively buoyant jets

Governing Equations

The basic equations are

$$\frac{\partial u_i}{\partial x_i} = 0, \quad (1)$$

$$u_j \frac{\partial u_i}{\partial x_j} = -\frac{1}{\rho_a} \frac{\partial P}{\partial x_i} + \frac{\partial}{\partial x_j} \left(\nu \frac{\partial u_i}{\partial x_j} - \overline{u'_i u'_j} \right) + \alpha g_i \Delta T, \quad (2)$$

$$u_j \frac{\partial T}{\partial x_j} = -\frac{\partial}{\partial x_j} \overline{u'_j \theta}, \quad (3)$$

$$u_j \frac{\partial \varepsilon}{\partial x_j} = \frac{\partial}{\partial x_j} \left[\left(\nu + \frac{\nu_t}{\sigma_\varepsilon} \right) \frac{\partial \varepsilon}{\partial x_j} \right] + \quad (4)$$

$$C_{\varepsilon 1} \frac{\varepsilon}{k} (P_k + G) - C_{\varepsilon 2} \frac{\varepsilon^2}{k},$$

$$u_j \frac{\partial k}{\partial x_j} = \frac{\partial}{\partial x_j} \left[\left(\nu + \frac{\nu_t}{\sigma_k} \right) \frac{\partial k}{\partial x_j} \right] + \quad (5)$$

$$\nu_t \left(\frac{\partial u_i}{\partial x_j} + \frac{\partial u_j}{\partial x_i} \right) \frac{\partial u_i}{\partial x_j} - \alpha g_i \overline{u'_j \theta} - \varepsilon,$$

where u_i is equal u , v or w , which are mean velocity components in x , y , z directions respectively, P is the intensity of pressure, ρ_a is the ambient fluid density, ν is the kinematic viscosity, $-\overline{u'_i u'_j}$ is the Reynolds stress, $-\overline{u'_j \theta}$ is the Reynolds diffusivity of heat, T is the temperature of jets, k is the turbulent kinetic energy, and ε is the dissipation rate of the turbulent kinetic energy. According to the Boussinesq eddy-viscosity concept that assumes that in analogy to the viscous stress in laminar flows, the turbulent stresses are proportional to the mean-velocity gradients, so the Reynolds stress and the Reynolds diffusivity of heat may be expressed as

$$-\overline{u'_i u'_j} = \nu_t \left(\frac{\partial u_i}{\partial x_j} + \frac{\partial u_j}{\partial x_i} \right) - \frac{2}{3} \delta_{ij} k, \quad (6)$$

$$-\overline{u'_j \theta} = \frac{\nu_t}{p_{rt}} \frac{\partial T}{\partial x_j}, \quad (7)$$

where ν_t is the eddy viscosity, and $\nu_t = C_\mu k^2 / \varepsilon$, p_{rt} is the turbulent Prandtl number, and it is a constant. P_k is the production of the turbulent kinetic energy and is defined in the following expression:

$$P_k = \nu_t \left(\frac{\partial u_i}{\partial x_j} + \frac{\partial u_j}{\partial x_i} \right) \frac{\partial u_i}{\partial x_j}. \quad (8)$$

The constants of the $k - \varepsilon$ model are

$$C_\mu = 0.09, \quad C_{\varepsilon 1} = 1.44, \quad C_{\varepsilon 2} = 1.92,$$

$$\sigma_k = 1.0, \quad \sigma_\varepsilon = 1.3, \quad p_{rt} = 1.0.$$

Boundary Conditions

1) Entry boundaries ($X = -2B$)

$$u = u_a, \quad v = w = 0, \quad T = T_a,$$

$$k_a = 0.06u_a^2, \quad \varepsilon_a = 0.06u_a^3/B,$$

where B is the width of diffuser.

2) Exit boundaries (its range changes with changing of length of diffuser)

$$\frac{\partial}{\partial x} [u, v, w, T, k, \varepsilon] = 0.$$

3) Symmetry plane ($y = 0$)

$$v = 0, \quad \frac{\partial}{\partial y} [u, w, T, k, \varepsilon] = 0.$$

4) Side boundaries (its range changes with changing of length of diffuser)

$$v = w = 0, \quad \frac{\partial}{\partial y} [u, T, k, \varepsilon] = 0.$$

5) Top boundaries (its range changes with changing of length of diffuser)

$$v = w = 0, \quad \frac{\partial}{\partial z} [u, T, k, \varepsilon] = 0.$$

6) Exit of buoyant jets boundaries ($-B/2 \leq X \leq B/2$)

$$u = \frac{1}{2} w_0, \quad v = 0, \quad w = \frac{\sqrt{3}}{2} w_0,$$

$$T = T_0, \quad k_0 = 0.06w_0^2, \quad \varepsilon = 0.06w_0^3/B$$

7) Bottom boundaries ($Z = 0$)

The universal law of the wall is used and may be expressed as

$$u_p / u_* = [\ln(y^+ E)] / K, \quad v_p = 0, \quad (9)$$

where u_p is the resultant velocity parallel to the wall, u_* is the resultant friction velocity, $y^+ = y_p u_* / \nu$ is the dimensionless wall distance, K is the von Karman constant, y_p is the distance between the first grid and wall, and E is a roughness parameter ($E = 9.0$ for hydraulically smooth walls). This law should be applied to a point whose y^+ -value is in the range $11.6 < y^+ < 100$. It is then sufficiently accurate in most situations. The areas near separation and stagnation points are exceptions, but they are usually small and exert little overall influence on the flow.

In the y^+ -region specified above, the turbulent kinetic energy k and the rate of dissipation ε may be expressed as

$$k_p = u_*^2 / \sqrt{c_\mu}, \quad \varepsilon_p = u_*^3 / (K y_p). \quad (10)$$

Mathematical Model

The above mathematical model can be generally expressed as a uniform form

$$2A\Phi_x + 2B\Phi_y + 2C\Phi_z = \Phi_{xx} + \Phi_{yy} + \Phi_{zz} + G. \quad (11)$$

Equation (11) is nonlinear, and for a grid unit, it may be linearized as follows:

$$2A^n\Phi_x^{n+1} + 2B^n\Phi_y^{n+1} + 2C^n\Phi_z^{n+1} = \Phi_{xx}^{n+1} + \Phi_{yy}^{n+1} + \Phi_{zz}^{n+1} + G^n, \quad (12)$$

where n and $n+1$ express the calculated values when the circulating number is n and $n+1$.

In the part grid, equation (12) is reduced through the Hybrid Finite Analytic Method to

$$\Phi_p = C_E\Phi_E + C_W\Phi_W + C_N\Phi_N + C_S\Phi_S + C_F\Phi_F + C_B\Phi_B + C_P G, \quad (13)$$

where

$$\begin{aligned} C_w &= \frac{E_A}{E} e^{-\bar{A}}, \quad C_E = \frac{E_A}{E} e^{-\bar{A}}, \quad C_s = \frac{E_B}{E} e^{-\bar{B}}, \\ C_N &= \frac{E_B}{E} e^{-\bar{B}}, \quad C_F = \frac{E_C}{E} e^{-\bar{C}}, \quad C_B = \frac{E_C}{E} e^{-\bar{C}}, \\ E_A &= \bar{A}/\bar{h}_i^2 sh\bar{A}, \quad E_B = \bar{B}/\bar{k}_j^2 sh\bar{B}, \\ E_C &= \bar{C}/\bar{l}_q^2 sh\bar{C}, \quad C_p = \frac{1}{E}, \\ E &= 2\bar{A}/\bar{h}_i^2 cth\bar{A} + 2\bar{B}/\bar{k}_j^2 cth\bar{B} + 2\bar{C}/\bar{l}_q^2 cth\bar{C}, \\ \bar{A} &= \frac{1}{2}[2Ah_i + (h_{i+1} - h_i)/\bar{h}_i], \quad \bar{h}_i = \frac{1}{2}(h_i + h_{i+1}), \\ \bar{B} &= \frac{1}{2}[2Bk_j + (k_{j+1} - k_j)/\bar{k}_j], \quad \bar{k}_j = \frac{1}{2}(k_j + k_{j+1}), \\ \bar{C} &= \frac{1}{2}[2Cl_q + (l_{q+1} - l_q)/\bar{l}_q], \quad \bar{l}_q = \frac{1}{2}(l_q + l_{q+1}). \end{aligned}$$

where h , k and l are respectively the distances between two grid points in x , y , z direction.

ANALYSIS OF RESULT

The five cases have been calculated for $F_j = 72.2$, $L = 4B$ and R varying from 0.2 to 0.6, in which F_j is the discharge densimetric Froude number ($F_j = T_a W_0^2 / [(T_0 - T_a) g B]$), L is length of slot, B is the slot width and R is the ratio ambient velocity to jet exit velocity.

Flow Behavior

Figure 2 shows the velocity vectogram of symmetry plane for $R = 0.2$. Figure 2 shows the essential features of the jets are fully three-dimensional and it is difficult to visualize. The most striking feature is the transition from an initially inclined jet through a bending phase during which the buoyant jet becomes approximately parallel with the free stream. There is some slight acceleration of the flow in the bending over region because of the wake effect of the slowing-moving fluid entrained in the lee of the jet. The smaller the value of R is, the more easily a vortex is formed. Because of the continuity of stream, the ambient flows on each side of the centerline must meet at some point downstream and the flow spreads upward like a source.

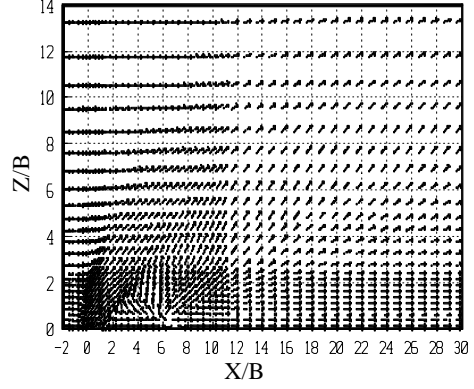


Figure 2: Velocity vectogram of symmetry plane for $R = 0.2$

A Vortex Pair to be Formed

On the basis of finite length line perpendicular buoyant jets in cross flows, a vortex pair aligned with the flow has been revealed (HAN and LI, 2000). For the finite length line inclined buoyant jets in a crossflow, the authors calculate five cases with the R varying from 0.2 to 0.6. The contour of temperature T at $X/B = 12$, $X/B = 24$, $X/B = 28$ (Figure 3, Figure 4, Figure 5, Figure 6 and Figure 7) show a vortex pair is also formed when R is smaller than 0.5, and it is not formed when R is larger than 0.5. The reason for it is that, smaller R can increase the force that the ambient flows on each side of centerline of diffuser flow to the plane of symmetry and the force that jet entrains environmental fluid, which cause to be formed a vortex pair easily. The distance between center of vortex and $x=0$ decreases, the distance between center of vortex and the plane of symmetry increases, and the height of center of vortex increases, with decreasing of R . When the R is a constant, the distance between center of vortex and the plane of symmetry will finally keep a constant, while the height of center of vortex will slightly increase because of the buoyant. Figure 7 indicates a kidney shape is formed. This is because jet for larger R discharging from jet exit is bending so fast that the force entraining environmental fluid is too small to form a vortex. From Figure 3 to Figure 7, we can see that the distance between center of vortex and plane of symmetry is related to R . The relational graph between them is showed in Figure 8, and the relational expression is

$$Y/B = 0.5R^{-1.31}. \quad (14)$$

A Flowing Structure of Horseshoe Shape

The contour of temperature T at $Z/B = 3$ for $R = 0.2$ is shown in Figure 9. Figure 9 shows that the ambient flows on each side of the centerline flow to the plane of symmetry and form a hoof shape in the lee of the jet, this is the mechanism that the cross flow is blocked by the jet.

CONCLUSIONS

The numerical solutions here for the finite length line inclined positively jets in cross flows have provided insight into the dynamics of this three-dimensional flow. The simulations reveal a vortex pair aligned with the flow what is related to R . For smaller values of R , the vortex pair can be easily formed. For $R > 0.5$, the vortex pair cannot

be formed. The model predicts that the position of center of vortex is related to R . The relational expression on the distance between center of vortex and the plane of symmetry and R is given.

REFERENCES

HU, J. M. and HAN, H. L., (2004), "Numerical study on behavior of finite length line inclined positively buoyant jets in cross flows", *J. of Hydrodynamics*, **19**, 275-280.

HAN, H. L. and LI W., (2000), "Influences of diffuser length on the buoyant jets in cross flows", *J. of Hydrodynamics*, **15**, 511-517.

JIRKA, G.H., (1982), "Multiport diffusers for heat disposal", *J. of Hydr. Div. ASCE*, **108**, 1425-1446.

LI, W., (2000), *Hybrid Finite Analytic Method of Viscous Fluid*, Science Press, Beijing, China.

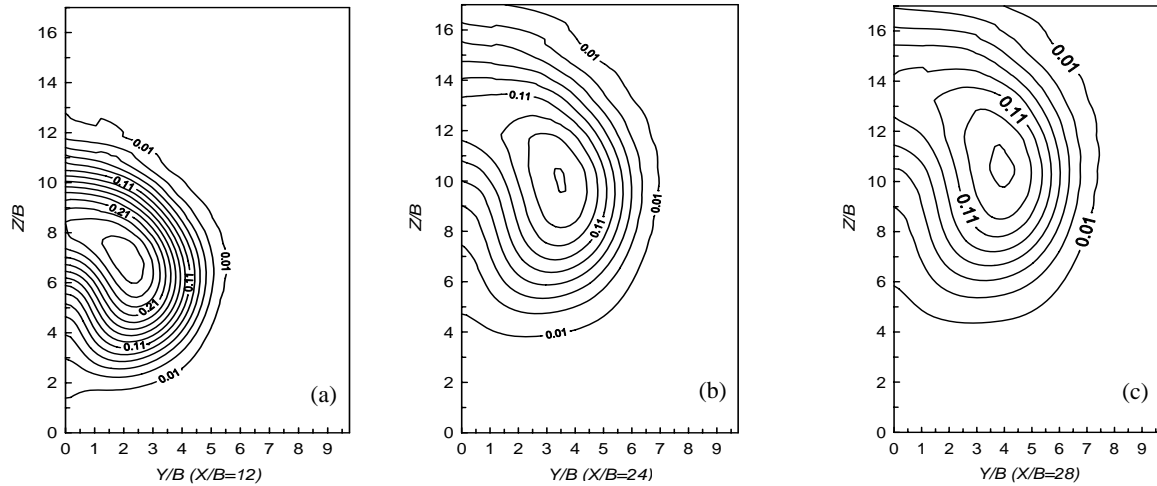


Figure 3: Temperature contours at different planes which parallel with $x=0$ and $R=0.2$

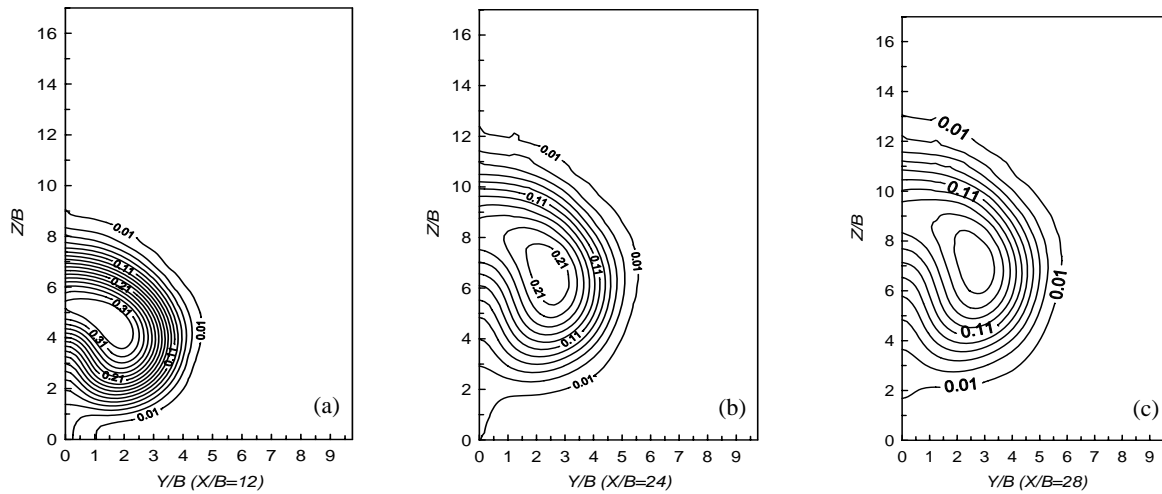


Figure 4: Temperature contours at different planes which parallel with $x=0$ and $R=0.3$

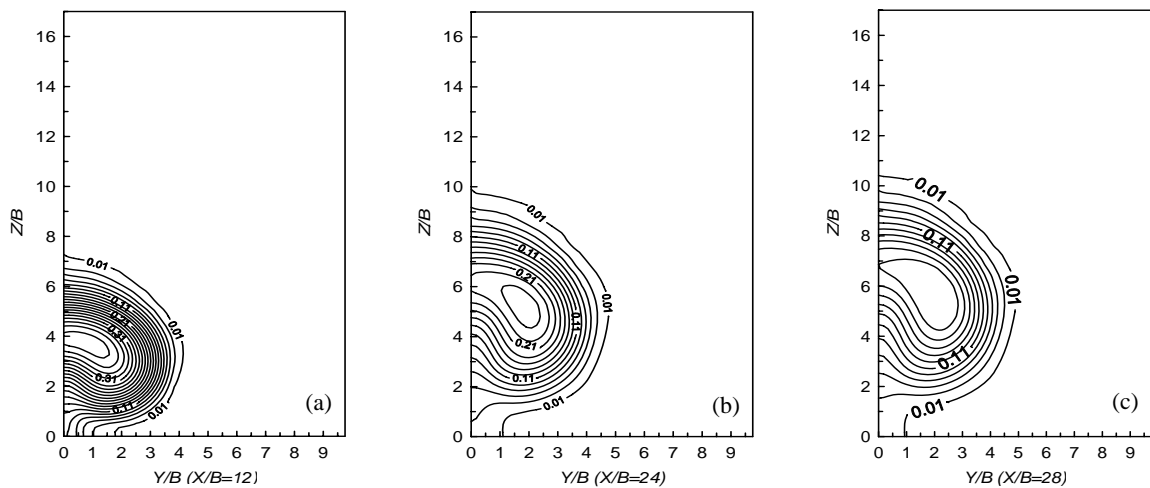


Figure 5: Temperature contours at different planes which parallel with $x=0$ and $R=0.4$

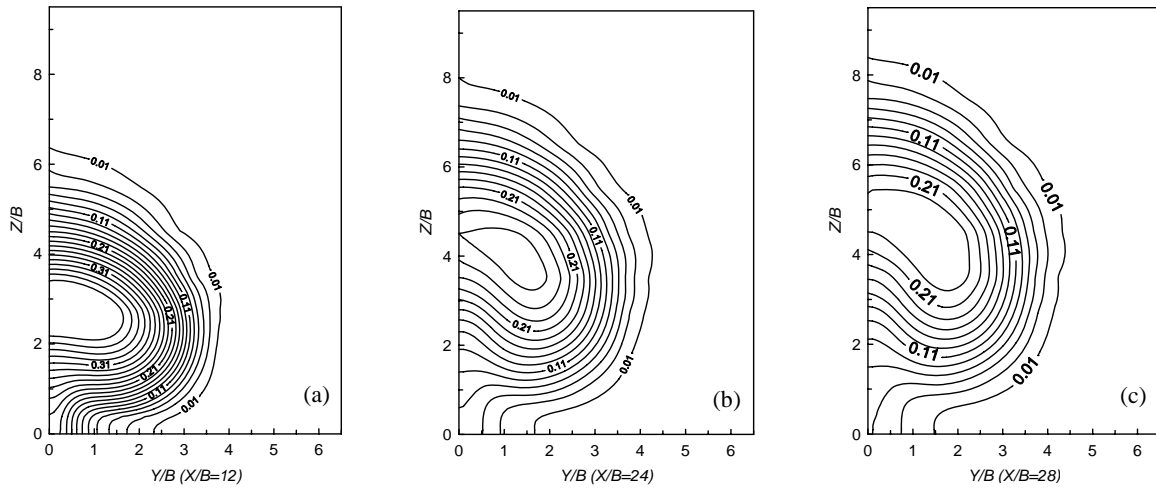


Figure 6: Temperature contours at different planes which parallel with $x=0$ and $R=0.5$

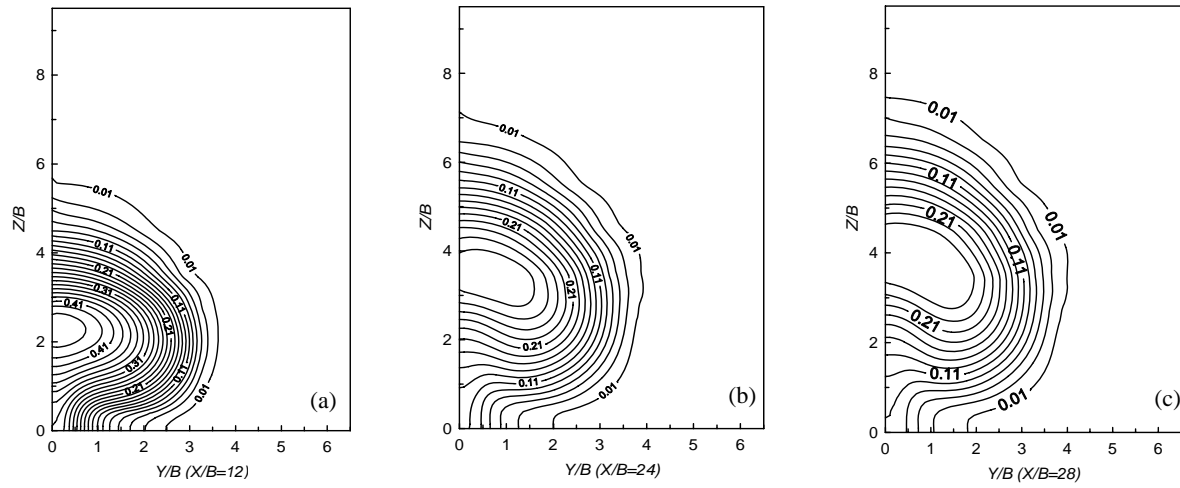


Figure 7: Temperature contours at different planes which parallel with $x=0$ and $R=0.6$

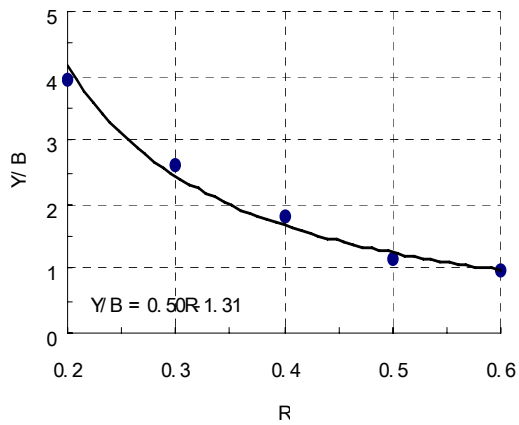


Figure 8: The relational graph on the distance between center of vortex and plane of symmetry and R

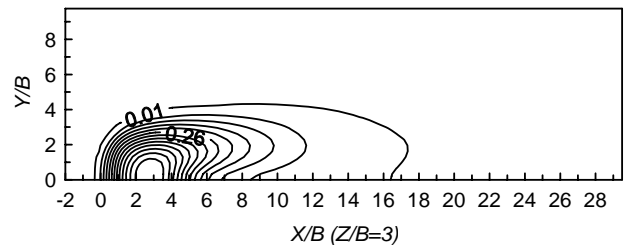


Figure 9: Temperature contour at $Z/B=3$ for $R=0.2$